

PRODUCTION MILLER-CYCLE NATURAL GAS ENGINE

1.0

As a total energy supply system, the cogeneration system has become part of building construction. Natural gas-fueled engines are used to generate electricity, and cooling water and exhaust heat energy are now recovered to supply hot water throughout the building. The total energy efficiency is in the neighborhood of 80 to 90 percent depending on the size of power generation. Gas companies in Japan have been developing systems for better fuel efficiency and lower exhaust emissions for more than a decade. Technology development continues while the number of production units has increased, as shown in Figure 1.0.1.

Engineers at Tokyo Gas Co., Ltd., and Yanmar Diesel Engine Co., Ltd. [Tsukida et al.] reported development results of a cogeneration system powered by an efficient natural gas engine. They have investigated Miller-cycle engine concept for several years^{1,2,3,4,5} and have now put the technology into a commercial application. To accomplish this development within the limited time frame of one year, they employed

Note: Name in bracket designates references at end of this report

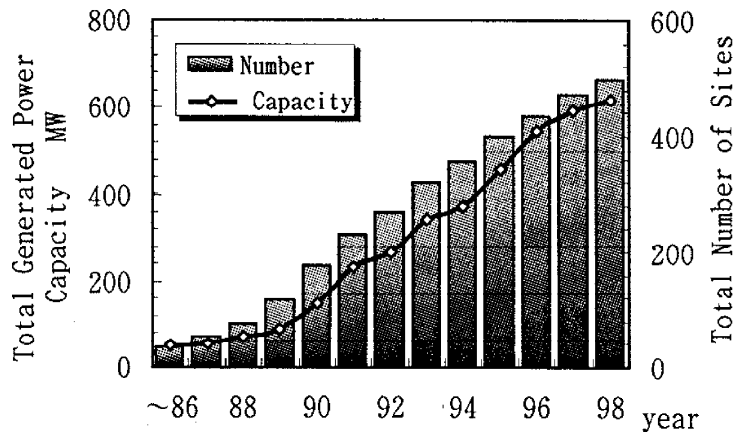


Figure 1.0.1

THE NUMBER OF COGENERATION SITES AND TOTAL POWER GENERATION CAPACITY IN THE MARKET OF TOKYO GAS [Tsukida et al.]

the relatively simple approach of late intake valve closure to increase the expansion ratio (13.3). With this approach, no significant engine modifications were necessary. Therefore, the prototype engine could be sufficiently tested for evaluating both reliability and durability before the final production engine design was completed. A 23.15-liter natural gas engine with Miller-cycle technology achieved 36.1 percent brake thermal efficiency, and the cogeneration system produced 300 kW of electric power. The total system including the heat recovery system achieved 83.5 percent energy efficiency. Regarding the engine durability, late-intake valve closure tends to have the reversed intake mixture into the

intake port which was of concern for developers because some lubricant-originated deposits accumulated. However, no serious problem was found during a 2000-hour operation under full load.

1.1 DEVELOPMENT OF A MILLER-CYCLE ENGINE FOR A NATURAL GAS COGENERATION UNIT [Tsukida et al.]

Cogeneration units powered by a natural gas engine have been produced in Japan for electric power generation capacity ranging from 15 to 4000 kW. The most popular range is 300 to 1000 kW, and the engine size ranges from 150- to 200-mm bore. Either stoichiometric-burn engine with a three-way catalyst or lean-burn technology has been used for emissions control. In recent years, lean-burn engines have increased production numbers because of higher thermal efficiency without after-treatment devices for control of exhaust gas emissions. However, control of nitrogen oxides (NOx) with only lean-burn technology will become more difficult as more stringent emissions standards come into effect. On the other hand, the stoichiometric-burn engine with a three-way catalyst can decrease NOx still lower and produce high exhaust gas energy

¹ See Chapter 3, Improvement of Natural Gas Engine Performance and Emissions, *ENGINE TECHNOLOGY PROGRESS IN JAPAN - Alternative Fuels and Engines*, published by ITEP in April 1998.

² See Chapter 1, Miller-Cycle Natural Gas Engine, *ENGINE TECHNOLOGY PROGRESS IN JAPAN - Alternative Fuels and Engines*, published by ITEP in July 1997.

³ See Chapter 2, Miller System and Supercharging for Gas Engines, *ENGINE TECHNOLOGY PROGRESS IN JAPAN - Alternative Fuels and Engines*, published by ITEP in April 1997.

⁴ See Chapter 1, Advanced Natural Gas Engine Technology Development, *ENGINE TECHNOLOGY PROGRESS IN JAPAN - Alternative Fuels and Engines*, published by ITEP in October 1996.

⁵ See Chapter 3, High Efficient Natural Gas Engines, *ENGINE TECHNOLOGY PROGRESS IN JAPAN - Alternative Fuels and Engines*, published by ITEP in July 1995.

for sufficient heat recovery. The total cogeneration efficiency is more than 80 percent. However, power generation efficiency is not as good as that of a lean-burn engine.

The recent changes that have been made in the legislative regulations allow a natural gas engine to be used for both main power generation and emergency power generation. Thus, the engine is now required not only to emit low NO_x when it is used as the main power generation, but also to have high load response (i.e., idle to full load) when it is used as an emergency power unit.

Based on these issues, engineers developed a stoichiometric-burn natural gas engine to adopt the Miller-cycle concept in order to increase thermal efficiency and re-

duce NO_x simultaneously. Performance of such an engine is now acceptable for cogeneration application and meets durability requirements.

1.1.1 Production Development

A 23.15-liter production natural gas engine was modified for testing the Miller cycle with various expansion ratios. Table 1.1.1 lists the engine specifications. The expansion ratio was increased by closing an intake valve either at an early timing or a later timing. The engine operating conditions were 324 kW steady state brake power and 1.12 MPa brake mean effective pressure (BMEP) at 1500 rpm (for 50 Hz application). Intake charge temperature was set at 313°K.

Table 1.1.1
THE ENGINE SPECIFICATIONS [Tsukida et al.]

		Baseline Otto Cycle	Tested Miller Cycle
Type		Spark-Ignited 4-Stroke Cycle	
Cylinders x Bore x Stroke (mm)		6 x ϕ 170 x 170	
Displacement Volume (liter)		23.15	
Fuel		Natural Gas : LHV=41.6 MJ/Nm ³ 88.5% - CH ₄ , 4.6% - C ₂ H ₆ 5.4% - C ₃ H ₈ , 1.5% - C ₄ H ₁₀	
Rated Power (kW/rpm)		220 / 1200	324 / 1500
BMEP (MPa)		0.95	1.12
Equivalence Ratio		1.0 with Three-way Catalyst	
Supercharging		Turbo-charger / Inter-cooler	
Pressure Ratio of Turbo-charger		1.6	1.8 ~ 2.8
Expansion Ratio (Geometric Compression Ratio)		10.3	10 ~ 18
Intake Valve Timing	I VO (deg. BTDC)	20	
	I VC (deg. ABDC)	40	- 60, 40 ~ 140
Mechanism of Low Compression Ratio		NA	(1) E I VC (2) L I VC

Figure 1.1.1 shows valve lift as a function of crank angle and the calculated intake charge mass flow rate. With the early intake valve closure (EIVC), the maximum valve lift amount only decreased because the cam profile was similar to that of the base engine. Peak intake charge mass flow rate was high so that the amount of intake charge became sufficient to operate the engine under the specified condition. Thus, a higher intake charge pressure needs to be matched with valve opening characteristics. Also, the valve train system needs some modifications to achieve proper valve operation for such as valve lift, valve seating velocity, valve spring constant, etc.

The later intake valve closure (LIVC) extended the period of the maximum valve lift. Intake charge flow reversed into the intake port after the piston passed bottom dead center (BDC). LIVC does not require significant modifications on the valve train system.

The effect of intake valve closure timing on the effective compression ratio and intake charge temperature (in the intake port) was evaluated, as shown in Figure 1.1.2, when the expansion ratio was set at 14.2. Due to the inertial charge effect of the intake charge, the effective compression ratio peaked at 40° crank angle (CA) ABDC. The effective compression ratio was about the same regardless of EIVC and LIVC and symmetrically decreased before and after the peak value. In the case of LIVC, the intake charge temperature increased because of the reverse flow. The increased intake charge temperature was of concern because combustion knock might occur.

Thermal efficiency significantly increased when the expansion ratio was increased regardless of EIVC or LIVC, as shown in Figure 1.1.3. Spark timing was advanced to the knock limit timing. Thus, the Miller-cycle concept that was demonstrated by increasing the expansion ratio

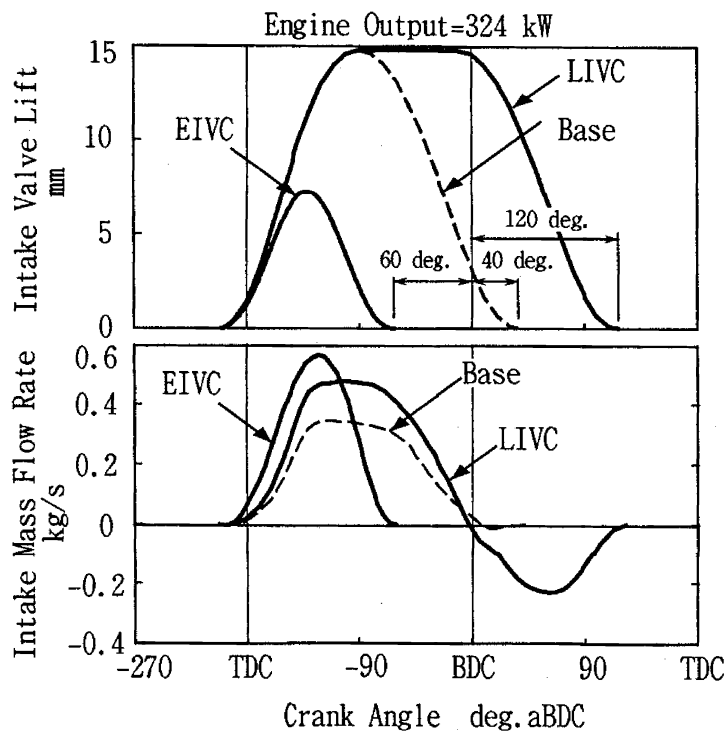


Figure 1.1.1

INTAKE VALVE LIFT AND INTAKE MASS FLOW RATE [Tsukida et al.]

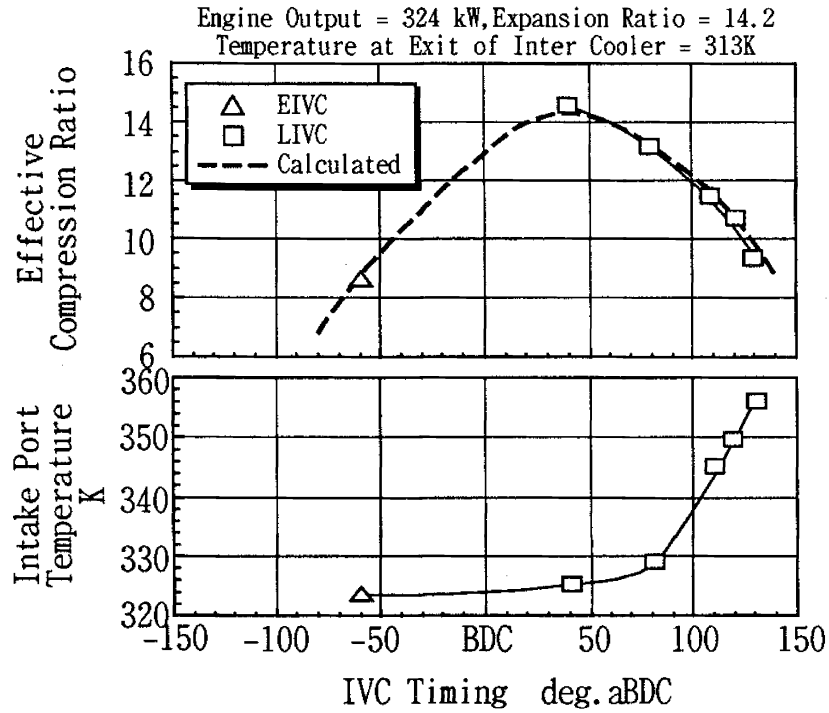


Figure 1.1.2
THE EFFECT OF INTAKE VALVE CLOSURE TIMING ON EFFECTIVE COMPRESSION RATIO AND INTAKE CHARGE TEMPERATURE AT AN INTAKE PORT [Tsukida et al.]

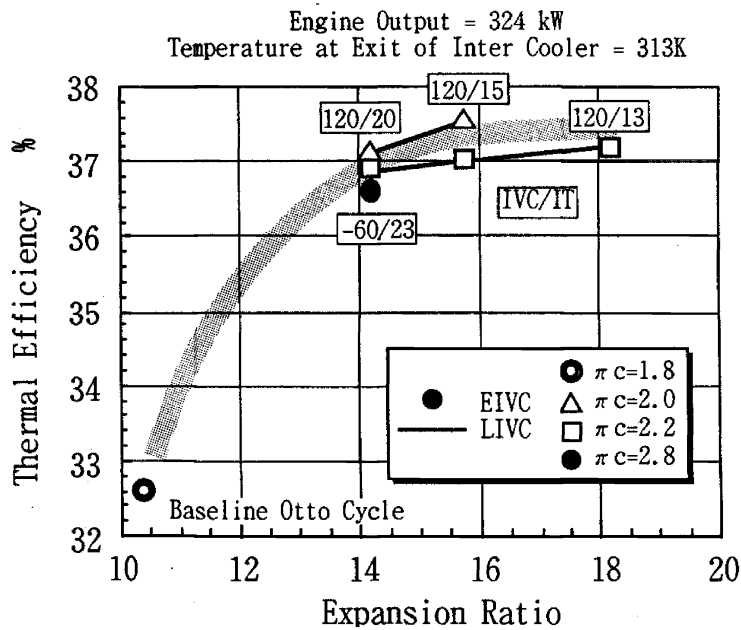


Figure 1.1.3
THE EFFECT OF EXPANSION RATIO ON BRAKE THERMAL EFFICIENCY [Tsukida et al.]

can effectively increase thermal efficiency.

1.1.2 Production Miller-Cycle Engine Development

The theory proved the improvement of thermal efficiency using a higher expansion ratio which was achieved by changing the intake valve closure timing to either an advanced or a retarded timing. To apply the Miller-cycle concept to a production engine, the engine reliability in addition to high thermal efficiency needs to be sufficiently high. The development time available for this particular engine was about one year. Therefore, engineers had to make decisions on the major engine specifications early in the project to allow them to test the engine for reliability. As a result, the LIVC method for increasing the expansion ratio was employed for production engine development. Compared to EIVC, LIVC required lower cost and fewer design changes. Table 1.1.2

lists the engine specifications.

Figure 1.1.4 schematically shows the engine setup. The engine was operated on premixed natural gas that was supplied upstream from the turbocharger. By use of a bypass valve with a feedback control, the air/fuel ratio was precisely controlled to maintain the stoichiometric ratio for the best three-way catalyst performance. The three-way catalyst was a metal-substrate made of stainless steel. The camshaft was designed and fabricated for the intake valve closure timings of 110 and 120°CA ABDC. The expansion ratio was 13.3 with IVC of 110°CA ABDC and 14.2 with IVC of 120°CA ABDC. These parameters were tested on the engine to evaluate thermal efficiency and combustion knock-limited engine load.

Knock Limit and Thermal Efficiency: Combustion knock was observed for trace knock in the cylinder pressure data. Using the trace knock, the knock-limit load was evaluated for the effect of various spark tim-

Table 1.1.2
PRODUCTION MILLER-CYCLE NATURAL GAS ENGINE SPECIFICATIONS [Tsukida et al.]

		Miller Cycle Gas Engine (Yanmar Diesel 6NHLM-ST)	
Type		Spark-Ignited 4-Stroke Cycle	
Cylinders x Bore x Stroke (mm)		6 x ϕ 165 x 185	
Displacement Volume (liter)		23.73	
Rated Power (kW/rpm)		324 / 1500	
BMEP (MPa)		1.09	
Equivalence Ratio		1.0 with Three-way Catalyst	
Supercharging		Turbo-charger / Inter-cooler	
Pressure Ratio of Turbo-charger		1.8	
Intake Valve Timing	I VO (deg. BTDC)	28	
	I VC (deg. ABDC)	- 110	- 120
Expansion Ratio (Geometric Compression Ratio)		13.3	14.2

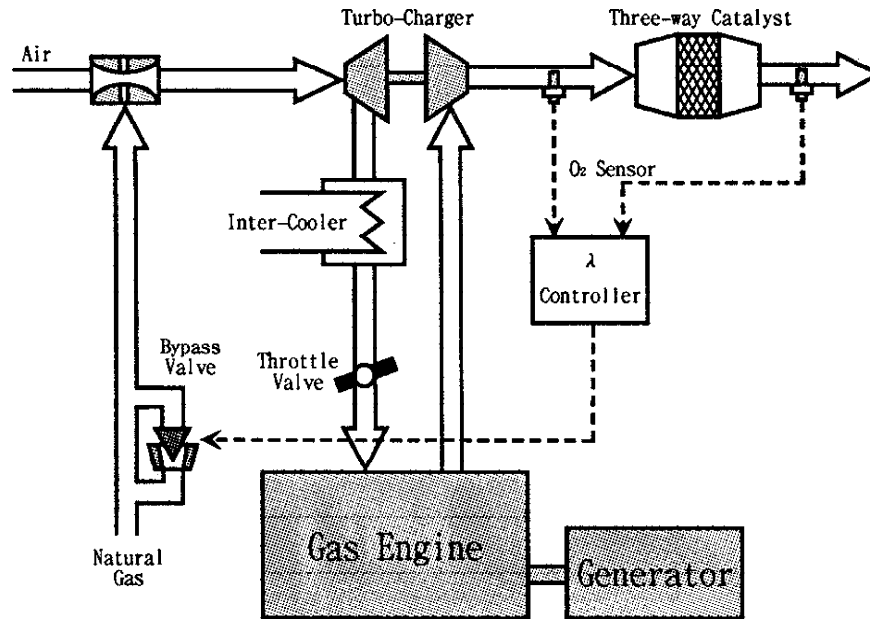


Figure 1.1.4
ENGINE SETUP [Tsukida et al.]

ings relative to that under the rated power condition. When the spark timing was the same, IVC of 120°CA ABDC with a 14.2 expansion ratio produced lower knock-limit load than that of 110°CA ABDC with a 13.3 expansion ratio, as shown in Figure 1.1.5. This difference could be made by the difference in the effective compression ratio between the two IVCs. IVC of 120°CA ABDC with a 14.2 expansion ratio resulted in 0.4 higher effective compression ratio. Also, the intake charge temperature raised (about 5 ~ 10°K) by the reverse flow probably affected this result. With IVC of 120°CA ABDC with a 14.2 expansion ratio, however, thermal efficiency was higher by about 1 point compared to that with 110°CA ABDC with a 13.3 expansion ratio, and the effect of spark timing was small.

The engine used for a cogeneration unit is required to have good durability. The engine is mostly operated under full load. The maintenance interval of the piston crown for deposit removal is 4000 ~ 8000 hours. Thus, the spark timing was set at an

appropriate timing considering lubricating oil deposits accumulated on the piston crown which tend to introduce combustion knock. The knock-limit load was therefore 115 percent when the intake charge temperature was 318°K. Therefore, with IVC of 120°CA ABDC with a 14.2 expansion ratio, the spark timing was set at 13°CA BTDC. Thermal efficiency was 36.9 percent. A 14.5°CA BTDC spark timing was set for IVC of 110°CA ABDC with a 13.3 expansion ratio. Thermal efficiency was 36.1 percent.

Load Response Characteristics: When the cogeneration unit is operated independently from the commercial electric power system, the unit is required to produce a certain power in a short time from idle. A turbocharged engine inherently has turbo-lag during power increase from the time when the engine is operated under the naturally-aspirated condition until the turbo-charger has become fully functional to increase the intake charge pressure. An engine that produces higher thermal efficiency tends to have poor load response character-

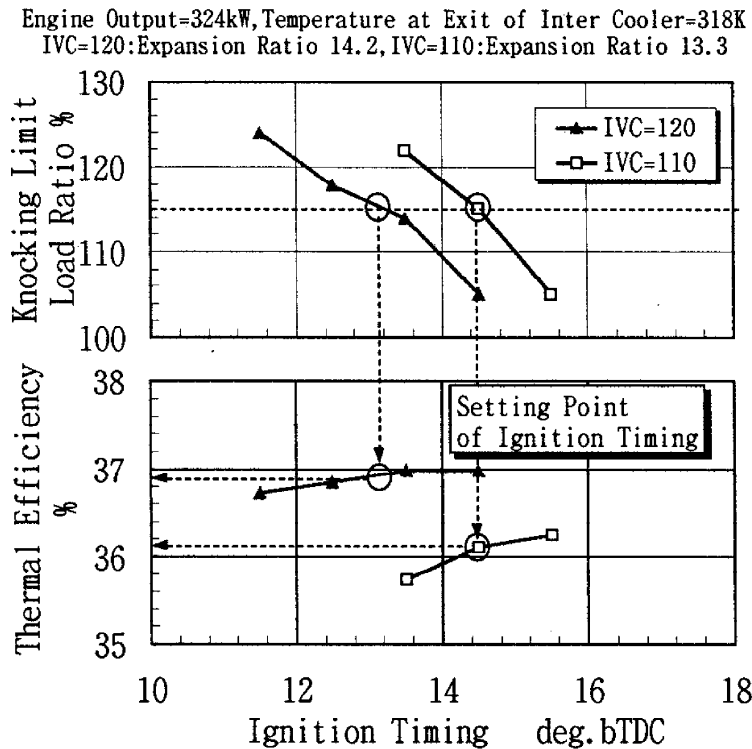


Figure 1.1.5

THE EFFECT OF SPARK TIMING ON KNOCK-LIMIT LOAD AND THERMAL EFFICIENCY [Tsukida et al.]

istics because the intake charge pressure is generally high.

Figure 1.1.6 shows the load response characteristics of either IVC of 110°CA ABDC or IVC of 120°CA ABDC. The turbocharger was the same type for both cases. The difference between the turbocharger boost pressure and the intake manifold pressure is lower in the case of IVC of 120°CA ABDC. From the thermal efficiency point of view, the smaller difference is advantageous. However, the load response is better if the difference is greater because a throttle valve is used to increase load. At idle, the engine is operated under naturally-aspirated conditions. So the intake charge relies on atmospheric pressure. Generally if the engine can produce a certain power when the intake manifold pressure is -10 kPa, the cogeneration unit is sufficiently powered even under cold conditions. With IVC of 120°CA ABDC, the power at -10 kPa

is about 120 kW which is 37 percent of the rated power. IVC of 110°CA ABDC could produce about 50 percent of the rated power or 160 kW. Therefore, the production engine used IVC of 110°CA ABDC, although the thermal efficiency is 0.8 points lower than that of IVC of 120°CA ABDC. Load response was taken as more important than engine performance at this time.

1.1.3 Cogeneration Package

The package was divided into two units. The main unit was equipped with a natural gas engine, electric generator, control panel, three-way catalyst, and exhaust heat recovery device, as shown in Figure 1.1.7. The sub-unit had a steam boiler, silencer, and cooling tower. The electric power generation capacity is 300 kW. The package was designed to be compact (0.07 m²/kW), and all units were assembled in one pack-

age. This all-in-one package method alleviated the initial installation process of the cogeneration system at a site.

Table 1.1.3 lists the cogeneration specifications. The Miller-cycle approach accomplished the objectives of a clean and highly efficient cogeneration system. The engine's

brake thermal efficiency was 36.1 percent, and the cogeneration unit's total package achieved 83.5 percent efficiency. Since the intake flow reverse occurs in the engine with late intake valve closure, deposits on intake port wall were of concern. Lubricating oil in the cylinder may be carried by the reverse flow and accumulate in the intake port. As of 2000s hour of engine operation under full load, however, there have not been any deposits on the intake port wall.

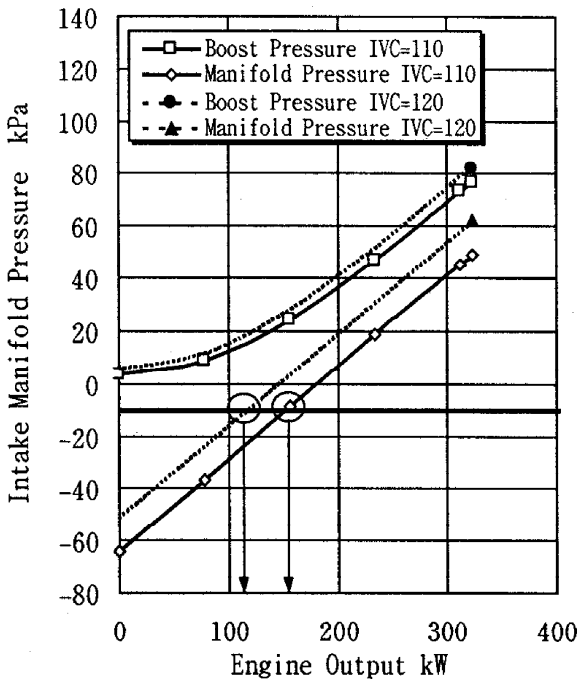


Figure 1.1.6

LOAD RESPONSE CHARACTERISTICS [Tsukida et al.]

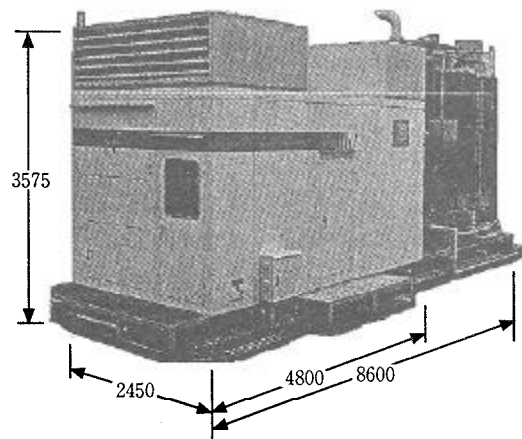


Figure 1.1.7

ALL-IN-ONE PACKAGE OF A COGENERATION UNIT [Tsukida et al.]

Table 1.1.3
COGENERATION SPECIFICATIONS [Tsukida et al.]

		Developed Miller Cycle Gas Engine Cogeneration System
Input / Fuel Consumption		877 kW / 76.0 m ³ N/h (Natural Gas supplied by Tokyo Gas)
Output / Efficiency	Generated Power	300 kW (50 Hz) / 34.2%
	Heat Recovery (Engine Jacket & Exhaust Gas)	252 kW (358K Hot Water) / 28.7%
		181 kW (0.78 MPa Saturated Steam) / 20.6%
NOx Emission		Under 40 ppm@O ₂ =0% Dry
Bearable Load Ratio (from idling)		50% - 150 kW